

SOURCE, PATH AND SITE EFFECTS ON STRONG GROUND MOTIONS FROM THE 2003 TOKACHI-OKI EARTHQUAKE SEQUENCE

**Tsutomu SASATANI¹, Takahiro MAEDA², Nobuo TAKAI³, Goro MIWADA⁴,
Gaku SHIMIZU⁵, Akio YAMAMOTO⁶, and Shinako NOGUCHI⁷**

ABSTRACT

The 2003 Tokachi-oki earthquake, a great interplate earthquake (Mw8.3), is the first M8 class earthquake in Japan since the dense strong-motion networks such as the K-NET and KiK-net have been deployed. We examine spatial distributions of velocity responses (damping factor $h=0.05$) with various natural periods for this earthquake by using the dense strong-motion network data. The short-period ($T=0.1\text{sec}$; $T=\text{natural period}$) velocity response distribution shows a typical feature for subduction-zone earthquakes; the high response values are observed along the Pacific coast of north Japan. This feature is explained by the S-wave attenuation structure beneath north Japan; that is, the path effect. On the other hand, the long-period ($T=20\text{sec}$) velocity response distribution shows a peculiar feature: at comparable distance, the response values in the northern part of the epicenter are higher than those in the south-western part. This peculiar feature is mainly explained by the source effect; the radiation pattern of long-period Rayleigh waves. We find various types of the site effects. A remarkable one is excitation of long-period basin surface-waves at large plains with thick sedimentary layers. The other remarkable one is nonlinear site response. We find mild nonlinear site response at a soft soil site located on flood plain deposits; the nonlinearity is confirmed by comparing the transfer functions for weak and strong motions using the downhole array data. The distinctive nonlinearity is also observed at a not-so-soft soil site located on reclaimed land during the largest aftershock; the accelerogram shows a spiky waveform.

Keywords: The 2003 Tokachi-oki earthquake, velocity response, nonlinear site response

INTRODUCTION

1

On September 26, 2003, the Tokachi-oki earthquake (Mj 8.0; magnitude after Japan Meteorological Agency, JMA) occurred south off Hokkaido (Fig. 1). This earthquake is a large interplate earthquake between the Pacific and Okhotsk plates, and the source area is almost the same as that of the 1952 Tokachi-oki earthquake (Mj 8.2). During the earthquake, long-period ground motion damaged huge oil tanks due to the sloshing phenomenon at Tomakomai about 200 km away from the epicenter. We have re-realized from this fact that long-period ground motion has potential to cause serious damage to high-rise and large-scale structures even at a long distance.

¹ Associate Professor, Faculty of Science, Hokkaido University, sasatani@ares.sci.hokudai.ac.jp

² Researcher, Faculty of Science, Hokkaido University, Sapporo 060-0810, Japan

³ Associate Professor, Graduate School of Engineering, Hokkaido Univ., Sapporo 060-8626, Japan

⁴ Graduate Student, Graduate School of Engineering, Hokkaido Univ., Sapporo 060-8626, Japan

⁵ Fukushima Prefecture Office, Fukushima 960-8670, Japan

⁶ Technical Center of OYO Corporation, Tsukuba 305-0841, Japan

⁷ Graduate Student, Faculty of Science, Hokkaido University, Sapporo 060-0810, Japan

Dense strong-motion networks have been deployed all over Japan after the 1995 Kobe earthquake (Mw6.9). K-NET (Kinoshita, 1998) and KiK-net (Aoi et al., 2000) of National Research Institute for Earth Science and Disaster Prevention (NIED) are representative ones in Japan; K-NET and KiK-net consist of more than 1000 and 550 stations, respectively. The 2003 Tokachi-oki earthquake is the first M8 class earthquake in Japan since the dense strong-motion networks have been deployed. This earthquake provides a good opportunity for studying seismic source, propagation path and site effects on strong ground motions for a large earthquake.

There exist various tectonic units in the north Japan subduction zone. The Pacific plate descends into mantle at the Kurile and Japan trenches, and volcanoes and a volcanic front (VF) exist in Hokkaido and north Honshu islands as shown in Fig. 1(a). These tectonic units construct a heterogeneous structure as shown in Fig. 1(b). In the figure, Q_s values (Q values for S-wave) at 1.5 Hz and 10Hz are given for the upper slab, lower slab, fore-arc side mantle wedge (FAMW) and back-arc side mantle wedge (BAMW); these are taken from Maeda and Sasatani (2001, 2006a). In the following discussions, we refer to these tectonic units.

In this study, we examine regional-scale characteristics of ground motion from the 2003 Tokachi-oki earthquake by using the K-NET, KiK-net and JMA strong ground motion data. First we show a preliminary examination of strong ground motions to illustrate the regional-scale characteristics. Then we derive the seismic source, propagation path and site effects on strong ground motions from spatial distributions and attenuation relations of velocity responses for various natural periods. Finally we show local site effects, that is, nonlinear site responses.

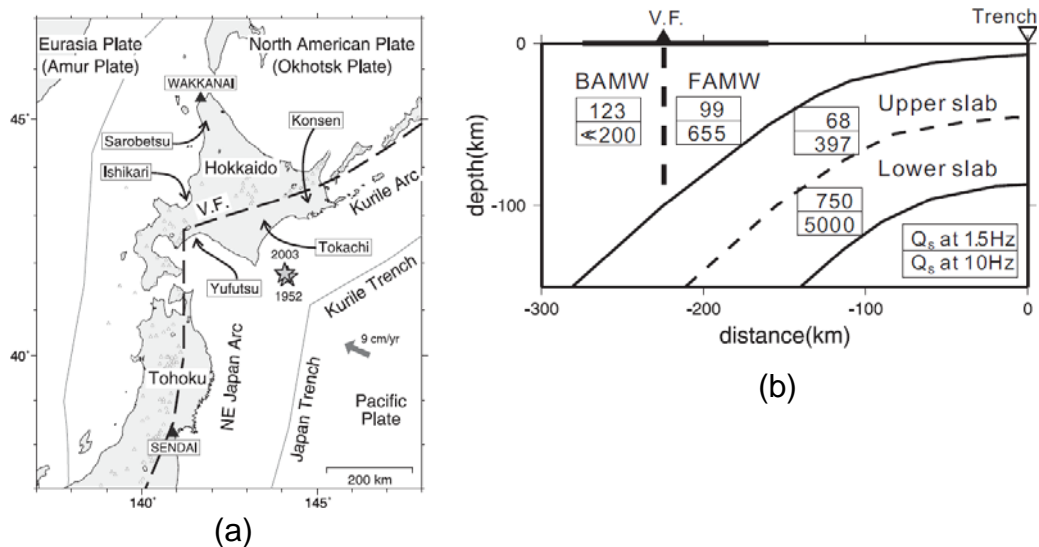


Figure 1. (a) A location map showing tectonic units in north Japan. Stars show epicenters of the 1952 and 2003 Tokachi-oki earthquakes. Solid triangles are JMA stations. Open triangles are quaternary volcanoes. V.F. indicates the volcanic front. Regions used in the text are also shown.

(b) Vertical cross section perpendicular to the trench axis beneath the eastern Hokkaido. Numbers in boxes indicate Q_s values at 1.5Hz and 10Hz in each zone.

SPATIAL DISTRIBUTIONS OF VELOCITY RESPONSES

Preliminary examination of strong ground motions

Figure 2(a) shows original strong motion seismograms at Wakkanai and Sendai from the 2003 Tokachi-oki main shock. The Wakkanai station is located at the northern tip of Hokkaido, and the Sendai station is located at Tohoku; these stations have nearly the same epicentral distances of about

450 km, but different epicenter-to-station azimuths (Fig. 1(a)). On the accelerograms, short-period waves predominate at Sendai, but strongly attenuate at Wakkanai. Though the peak amplitudes are comparable at these stations, long-period waves with a period of about 10 sec contribute to the peak amplitude at Wakkanai. On the contrary, long-period waves (surface wave) with periods of 10 to 20 sec predominate on the velocity seismograms; however, the peak amplitude at Wakkanai is about five times larger than that at Sendai. Figure 2(b) shows their velocity Fourier spectra (time window is about 120 sec). The spectral shapes greatly differ between the stations. The Wakkanai spectra have larger spectral amplitudes than those at Sendai for frequencies lower than 0.5 Hz while the Sendai spectra have larger amplitudes than the Wakkanai for frequencies higher than 0.5 Hz. These result from the source, path and site effects on strong ground motions as shown below. Figure 2 demonstrates that waves with different predominant periods contribute to PGA (peak ground acceleration) and PGV (peak ground velocity) depending on the epicenter-to-station azimuth. Therefore it is better to analyze velocity responses with various natural periods for studying spatial distribution features of strong ground motions.

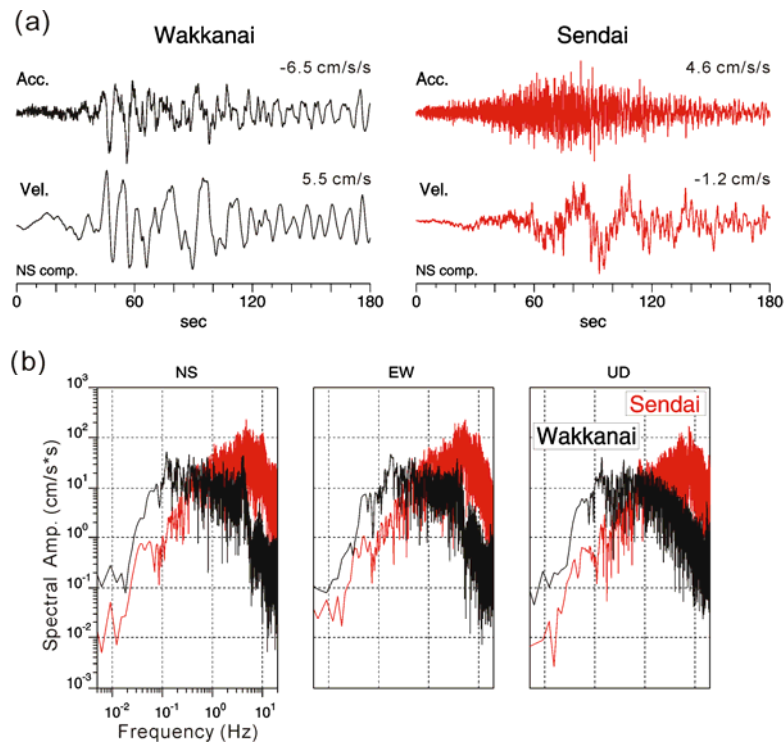


Figure 2. (a) Acceleration and velocity seismograms (N-S components) at Wakkanai and Sendai. (b) Their velocity Fourier spectra.

Spatial distribution features of velocity responses in north Japan

We calculate velocity responses (damping factor $h=0.05$) with various natural periods (T) for two horizontal components at a station. Then we make a vector sum for the two horizontal responses, and take the maximum value as the velocity response at the station. In the following discussions, we show only $T=0.1, 1.0, 10$ and 20 sec responses. The data consist of strong motion records in north Japan, obtained by the K-NET and KiK-net of National Research Institute for Earth Science and Disaster Prevention (NIED); the total number of stations used is 655.

Figure 3 shows the spatial distribution maps of the velocity responses for $T=0.1, 1.0, 10$ and 20 sec; concentric circles are epicentral distances at intervals of 100km. These maps show different features depending on the natural period; the response values increase with the periods all over northern Japan. We also make the attenuation relations of the velocity responses for $T=0.1, 1.0, 10$ and 20 sec (Fig. 4)

to help interpretation of the spatial distribution features. The data points are classified by a ratio of $L1/(L1+L2)$ where $L1$ is the fore-arc side distance and $L2$ is the back-arc side distance; the total epicentral distance (D) is divided into $L1$ and $L2$ at the volcanic front to simply consider the heterogeneous Qs structure (Fig. 1(b)) (Takai et al., 2004). We should note that the data are taken from different regions depending on the distance range. The data with $D < 250\text{km}$ are taken only from the Hokkaido region; those with $250 < D < 450\text{km}$, from the Hokkaido and Tohoku regions; and those with $D > 450\text{km}$, only from the Tohoku to Kanto region (see Fig. 3).

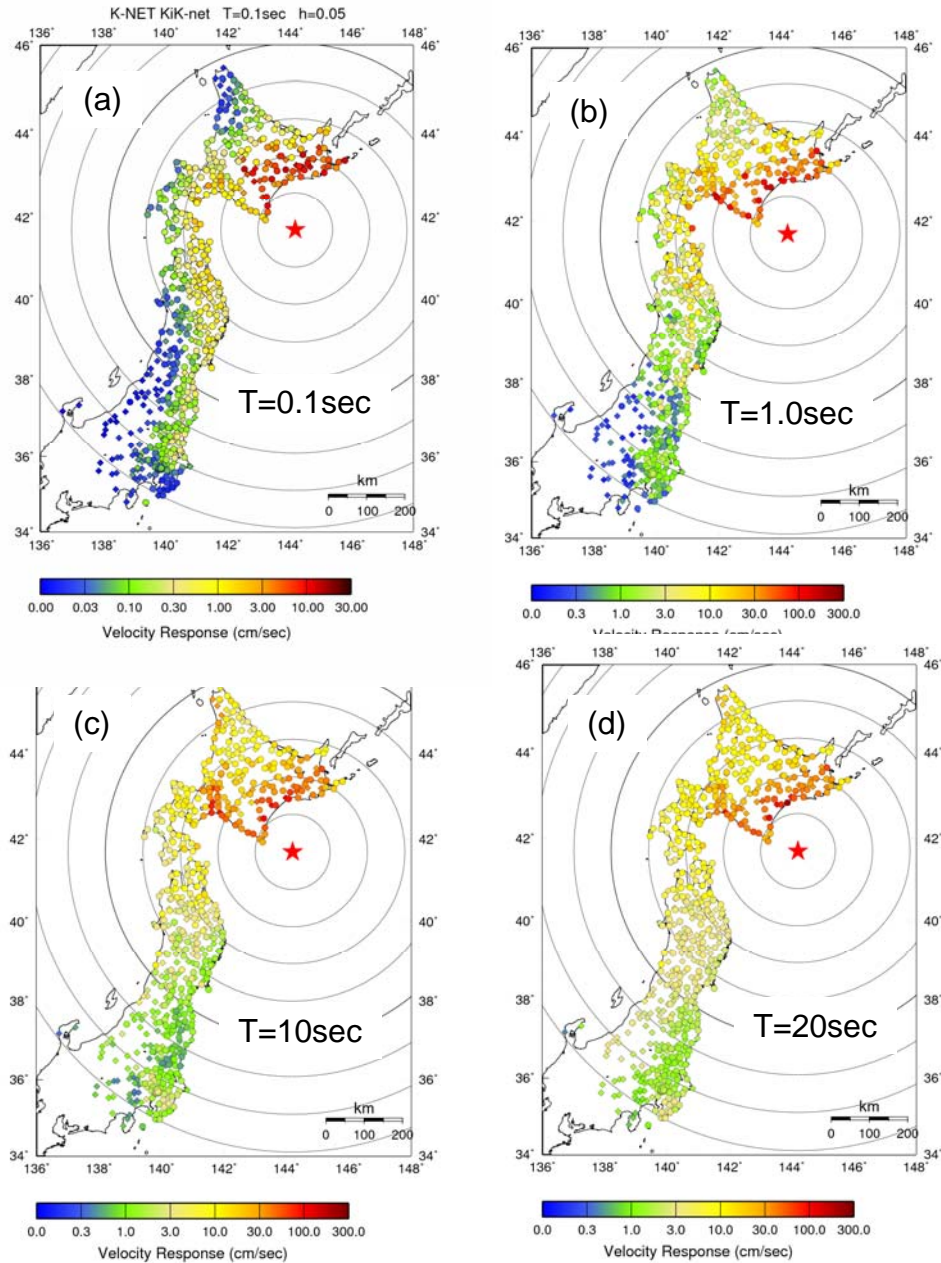


Figure 3. Spatial distribution maps of velocity responses during the 2003 Tokachi-oki earthquake for a damping factor of 5% and natural periods of (a) 0.1sec, (b) 1.0sec, (c) 10 sec, and (d) 20sec. Note that the color scale bars are the same except for the $T=0.1\text{sec}$ map.

In the $T=0.1\text{sec}$ attenuation relation, the large response values are observed at the fore-arc side of the volcanic front (VF), and the response values strongly decay with decreasing $L1/(L1+L2)$ ratios at the back-arc side of the VF. This is due to the heterogeneous Q_s structure shown in Fig. 1(b), and results in large scattering of the data points over two orders at distances larger than about 300km. One of the interesting points is that the data points at the fore-arc side of the VF change the decay rate around a distance of 300km. Seismic waves propagating to Hokkaido mainly pass through the mantle wedge, while seismic waves propagating to Tohoku mainly pass through the lower slab. Thus the decay-rate change of the attenuation relation at about 300 km suggests a different attenuation quality for the slab and mantle wedge.

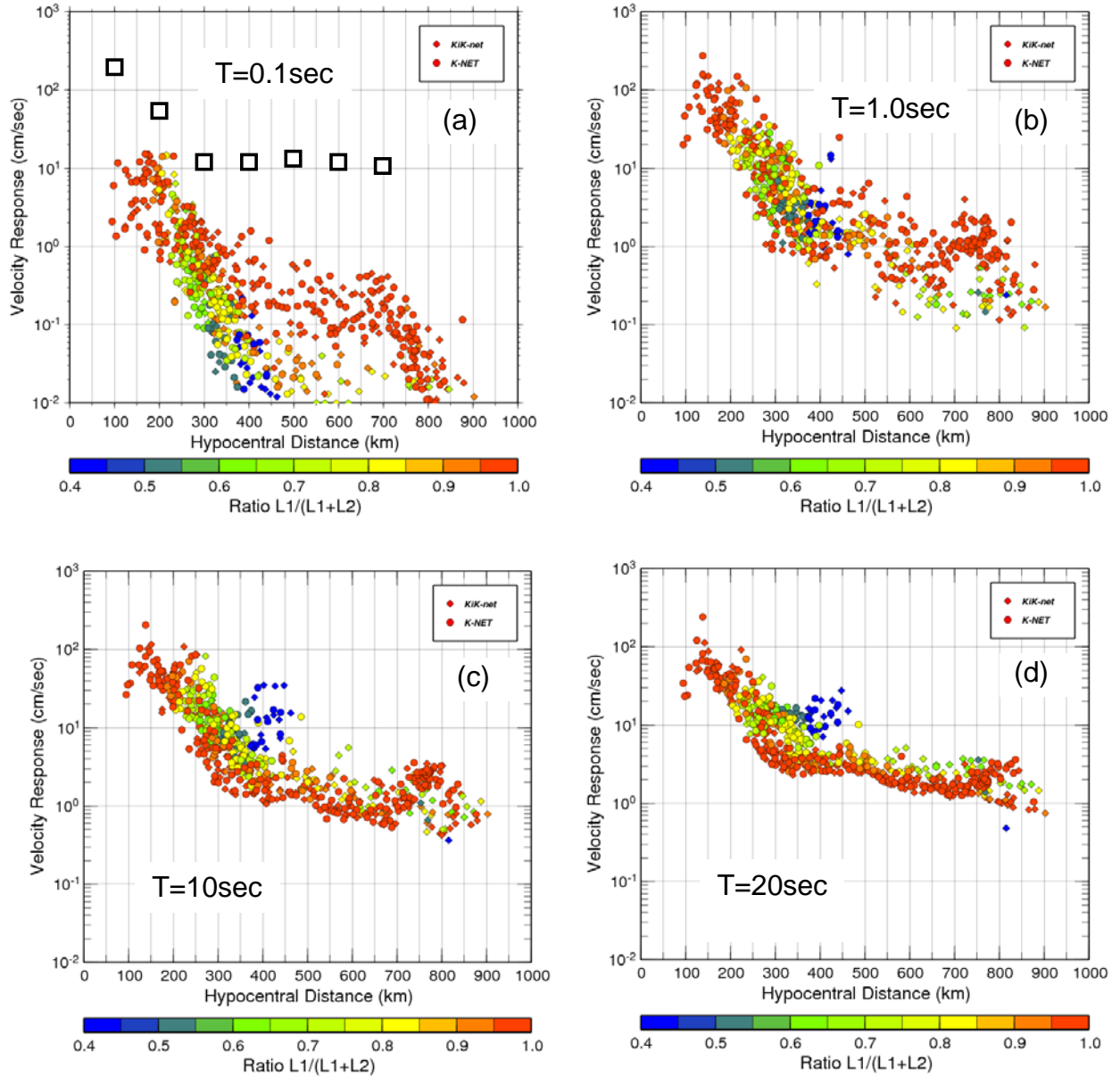


Figure 4. Attenuation relations of velocity responses for a damping factor of 5% and natural periods of (a) 0.1sec, (b) 1.0sec, (c) 10sec, and (d) 20sec. In (a), squares indicate the synthetic attenuation relation for the fore-arc side of the VF.

We try to explain the decay-rate change by the synthetic attenuation relation based on the Q_s structure model shown in Fig. 1(b). Figure 5 shows the Q_s models used in the calculation. A star at a distance of 0 km is the hypocenter of the 2003 Tokachi-oki earthquake. The right-hand side of the hypocenter corresponds to the FAMW of the Hokkaido region. The left-hand side of the hypocenter corresponds to the slab and the FAMW of the Tohoku region. We simply model the FAMW of the Tohoku region as shown in Fig. 5; the Tohoku FAMW has the same Q_s values as the Hokkaido FAMW. S-wave attenuation with a period of 0.1 sec is evaluated by geometrical spreading and anelastic attenuation (Q effect). The total attenuation effect due to the FAMW, and the upper and lower slab is evaluated based on the ray path passing through each zone. The geometrical spreading factor and ray path are calculated by dynamic ray tracing (Cerveny et al., 1977) for a one-dimensional velocity structure (an inset in Fig. 5) that roughly explains observed S-wave travel times for events occurring in the study region. The ray paths are calculated at an interval of 100 km for both sides of the hypocenter in Fig. 5. We assumed an isotropic radiation of short-period S waves. The synthetic attenuation relation for S wave with a period of 0.1sec is shown by open squares in Fig. 4(a). The synthetic data up to 200 km correspond to the Hokkaido region, and those for 300 km and over correspond to the Tohoku region. The synthetic relation roughly explains the observed decay rate change at the fore-arc side of the VF. From above discussions, we conclude that the spatial distribution of $T=0.1$ sec velocity responses and their attenuation relation are mainly caused by the path effect due to the heterogeneous Q_s structure beneath north Japan.

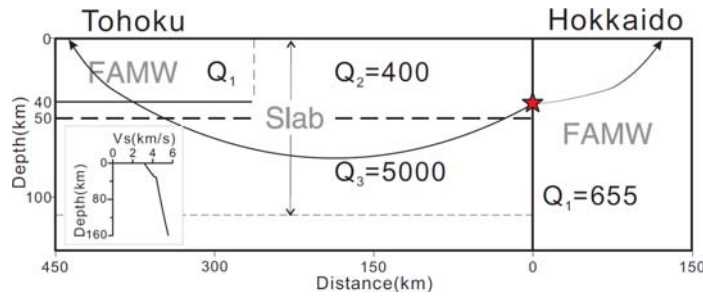


Figure 5. Q_s structure models toward the Hokkaido and Tohoku regions from the hypocenter of the 2003 Tokachi-oki earthquake (a red star). Solid curves indicate seismic rays calculated by ray theory assuming the 1-D velocity structure shown in the inset. The numerals are Q_s values at a period of 0.1 sec.

The scattering of data points in the attenuation relations considerably decreases with increasing natural period. The $L1/(L1+L2)$ ratios have no effects on the relations for $T=1.0$ sec, $T=10$ sec and $T=20$ sec; the data points with the smaller ratios show rather larger values around 400km in the $T=10$ sec and $T=20$ sec relations. This indicates that effects of the heterogeneous Q_s structure vanish for long-period seismic waves. However, the decay rate change in the $T=1.0$ sec attenuation relation at about 300km is attributed to high Q_s values in the lower slab as shown in Fig. 1(b); the data points are taken from the Tohoku to Kanto region at distances greater than 300km and these rays pass mainly through the lower slab.

In the $T=20$ sec attenuation relation, the decay rate changes around 300km. Maeda and Sasatani (2006b) examined velocity seismograms, and the spatial distribution and attenuation relation of peak ground velocity (PGV) from the 2003 Tokachi-oki main shock. They concluded that long-period waves with a period of about 20sec predominate on the velocity seismograms at most stations, and that long-period S-waves contribute to PGV at distances less than about 250km, while long-period surface waves (Rayleigh waves) contribute to PGV at distances larger than about 300km. Their conclusions easily explain the decay rate change at about 300km in the $T=20$ sec attenuation relation; the high decay rate at distances less than about 300km is due to S-waves and the low decay rate at distances

larger than about 300km is due to Rayleigh waves. We have to note that the factor in the decay rate change for the $T=20$ sec attenuation relation is different from that for the $T=0.1$ sec attenuation relation.

The $T=20$ sec attenuation relation shows considerably large scattering at distances from 250 to 450km; the larger responses are observed in the Hokkaido region as shown in Fig. 3(d). This scattering also appears in the PGV attenuation relation. Maeda and Sasatani (2006b) explained the PGV scattering by the radiation pattern of long-period Rayleigh waves, that is, the source effect. In Fig. 6, we cite their result that shows a comparison between the observed PGV pattern (U-D component) and synthetic radiation pattern of long-period (~ 20 sec) Rayleigh waves around a distance of 300km. Observed

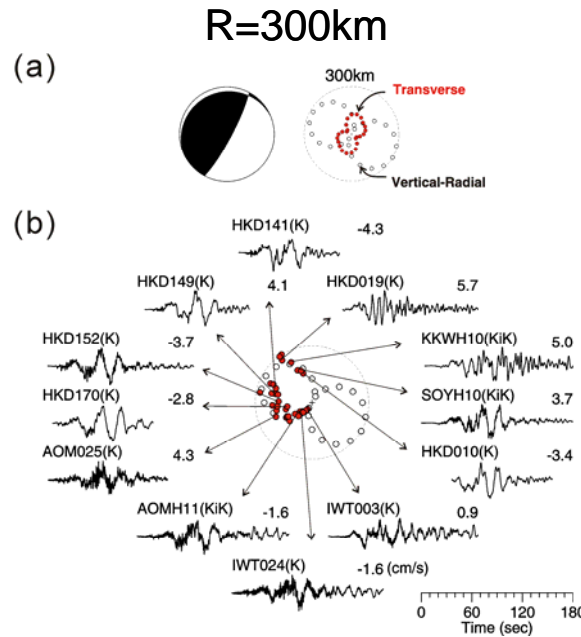


Figure 6. (a) Theoretical azimuth distributions of peak ground velocity amplitudes of Rayleigh and Love waves at an epicentral distance of 300km. The focal mechanism by Harvard University is also shown. (b) Azimuth distribution of peak ground velocity amplitudes (U-D component) at the epicentral distance of 300km; open circles are synthetic ones and solid circles, observed ones. Velocity seismograms observed at several stations are also shown.

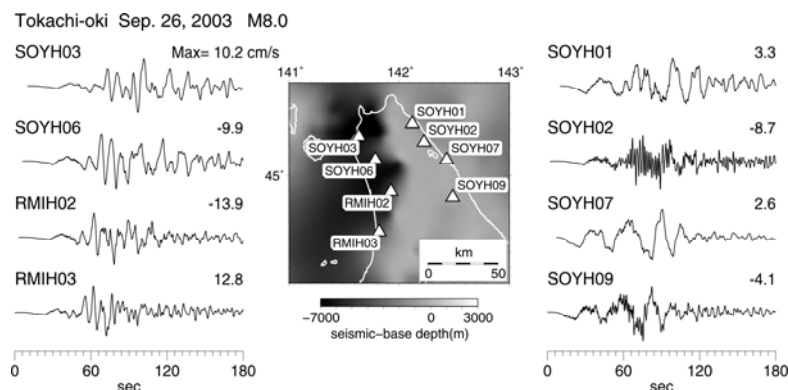


Figure 7. Velocity seismograms (N-S component) at northern Hokkaido. The inset map shows station locations and depths of upper boundary of $V_s=3.2$ km/s layer.

velocity seismograms are also shown in Fig. 6 at several stations; they have the predominant period of 20sec. Therefore we attribute the large scattering of the $T=20$ sec attenuation relation in the distance range of 250~450km to radiation pattern of Rayleigh waves, that is, the source effect.

The spatial distribution map of velocity responses for $T=10$ sec shows relatively large values at large sedimentary basins such as the Yufutu, Ishikari, Sarobetsu, Tokachi and Konsen plains in Hokkaido (the locations of these plains are shown in Fig. 1(a)). These large values result in the large scatterings at the corresponding distance in the $T=10$ sec attenuation relation. Among the large scatterings, a distinct one is observed at distances of about 400km; stations on the Sarobetsu plain contribute the large values in this distance range. Figure 7 shows a comparison of velocity seismograms at eight stations in the northern Hokkaido. An inset of Fig. 7 shows a depth distribution of seismic basement (Suzuki et al., 2004); the western side of the region with deep basement corresponds to the Sarobetsu plain. On the seismograms at the eastern stations, the 20sec period waves predominate, which are surface waves propagated from the epicenter. On the other hand, about 10sec period waves dominate on the seismograms at the western stations. It is certain that the 20sec period surface waves at the eastern stations are incident waves into northern Hokkaido. Thus the 10sec period waves at the western stations are surface waves transmitted into the Sarobetsu plain from the incident waves, that is, basin-transduced surface waves (Kawase, 1993). This is a kind of site effect which causes semi-regional scale anomalies in the spatial distribution map of velocity responses for $T=10$ sec (Fig. 3(c)). We also note that short-period waves (about 1.7sec) predominate at SOYH02. This is probably a local-scale anomaly caused by a small basin.

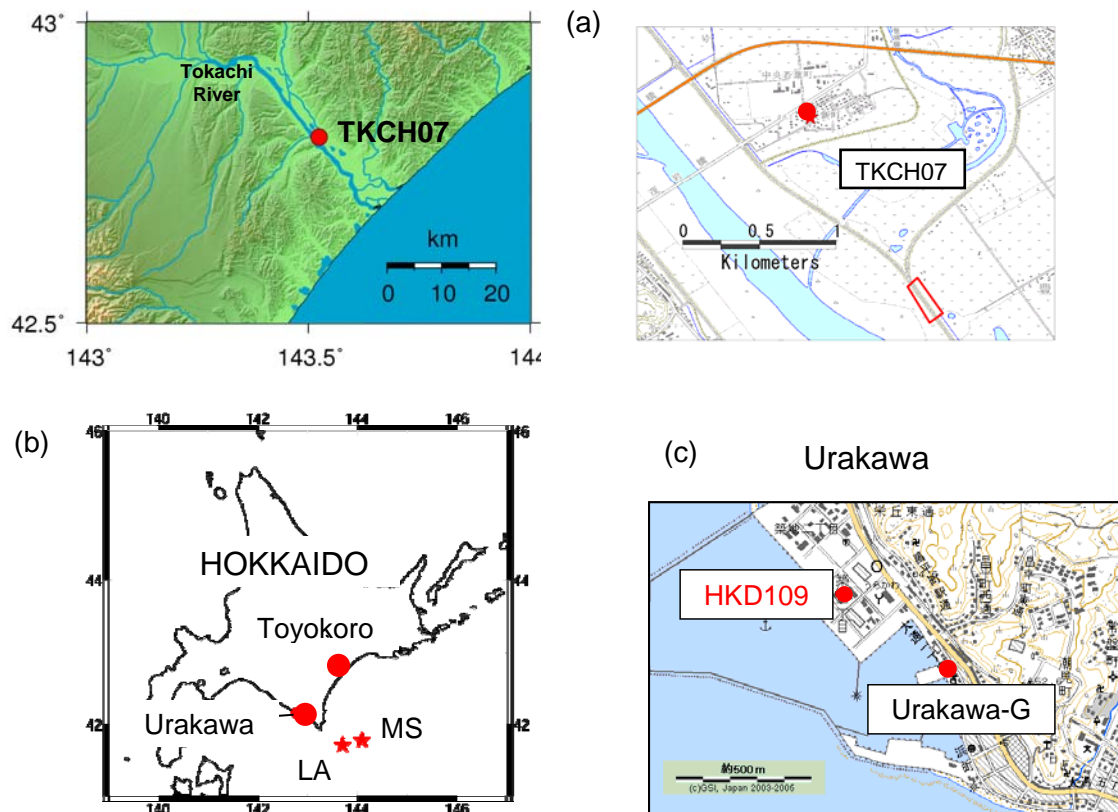


Figure 8. (a): Location map showing the Toyokoro site. (b): Toyokoro and Urakawa sites in Hokkaido. MS: Epicenter of the main shock, and LA: Epicenter of the largest aftershock. (c): Location map showing the Urakawa site.

NONLINEAR SITE RESPONSE

Liquefaction occurred at many port sites along the Pacific coast during the 2003 Tokachi-oki earthquake. Here we show nonlinear site responses based on strong motion records. Figure 8 shows study sites; Toyokoro and Urakawa sites.

Toyokoro site

The KiK-net TKCH07 station is located on flood-plain deposits in the Tokachi river (Fig. 8(a)). This station has a borehole seismometer at a depth of 100m. Figure 9(a) shows a comparison of S-wave surface-to-borehole spectral ratios (transfer functions) for weak and strong motion records. Grey lines are the spectral ratios for weak motions with surface PGA less than 100m/s/s, while a red line is that for strong motion with surface PGA of 400cm/s/s during the main shock. We can see that a shift to longer period of the fundamental frequency of the transfer function and reduction of the high-frequency level for the strong motion transfer function. Figure 9(a) clearly indicates nonlinear response at the TKCH07 site during the main shock (Sato et al., 1995; Wen et al., 1994).

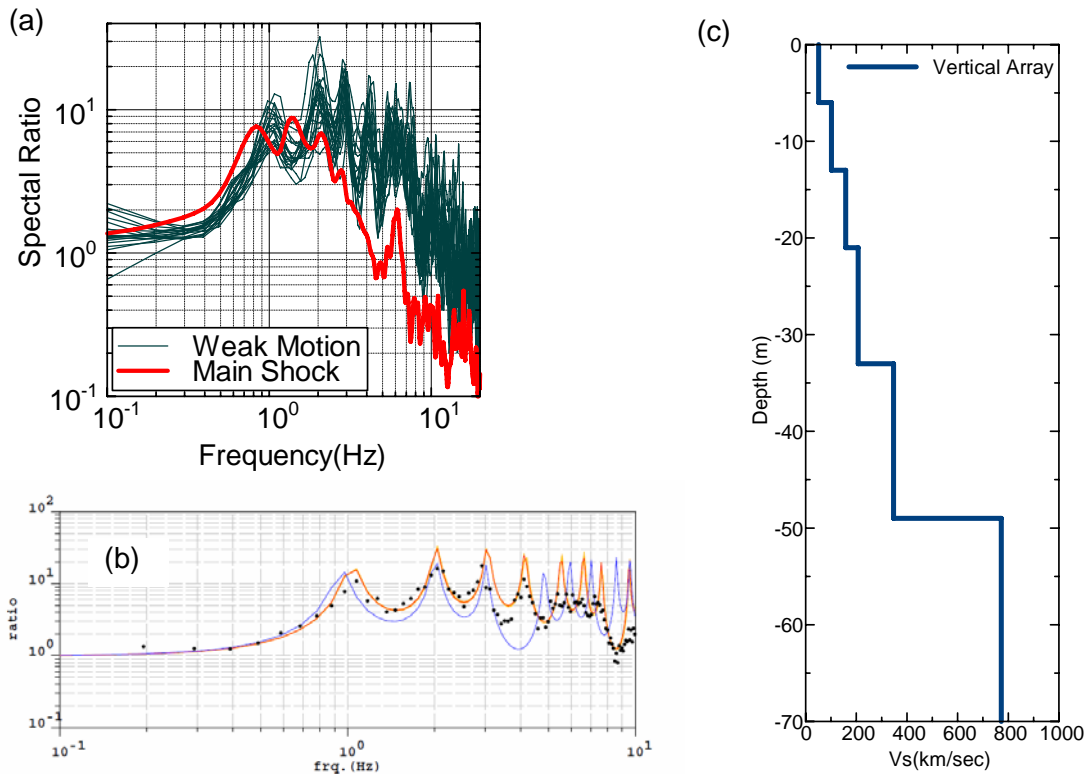


Figure 9. (a): Comparison of transfer functions for weak motions and strong motion (the main shock). (b): Comparison of the observed transfer function (dots) and theoretical one (red line) calculated from the S-wave velocity structure shown in the (c). The blue line in (b) is calculated from the PS-logging data.

We determined S-wave velocity structure from the transfer functions for weak motions. Figure 9(b) shows a comparison between the observed and theoretical transfer functions; the latter transfer function is calculated from S-wave velocity structure shown in Fig.9(c). The surface top layer, peat, has very small S-wave velocity of about 50m/s. The linear response based on this velocity structure and borehole accelerogram generates more than two times larger surface PGA compared with the observed one for the main shock. The equivalent linear response using the original SHAKE method generates about 70% surface PGA of the observed one. In this calculation, we use the standard

nonlinear soil parameters (modulus reduction and damping ratio curves for clay and sand), and the S-wave velocity structure and damping ratio determined from the transfer functions for weak motions. Thus the original SHAKE method is insufficient for predicting nonlinear soil response as noted by several authors (e.g. Hartzell et al., 2004); the SHAKE method with frequency-independent parameters over-damps the high frequency response.

Urakawa site

There are two stations on reclaimed land in Urakawa site; these are located on marine terrace. One is HKD109 of K-NET and the other is Urakawa-G of PARI (Port and Airport Research Institute); a distance between the two stations is about 500m (Fig. 8(c)). The Urakawa-G site was reclaimed earlier. The surface top layer has S-wave velocities of about 130m/s and 170m/s at HKD109 and Urakawa-G, respectively. The upper in Fig. 10 shows acceleration time histories at the two stations during the main shock. Both records have nearly the same PGA ($\sim 200\text{cm/s}^2$) and waveform. Weak motion records at the two stations keep these natures. On the contrary, waveforms of the two stations are extremely different during the largest aftershock (M7.1) that occurred about one hour and twenty minutes after the main shock (the lower in Fig. 10). A spiky waveform of HKD109 is characteristic. The spiky waveform is clearly observed in the Port Kushiro surface acceleration time history of the 1993 Kushiro-oki earthquake (Iai et al., 1995). Thorough analysis of this surface record by Iai et al. (1995) leaves no doubt that the spiky waveform is the result of nonlinear response, that is, the nonlinear dilatant behavior of the soil.

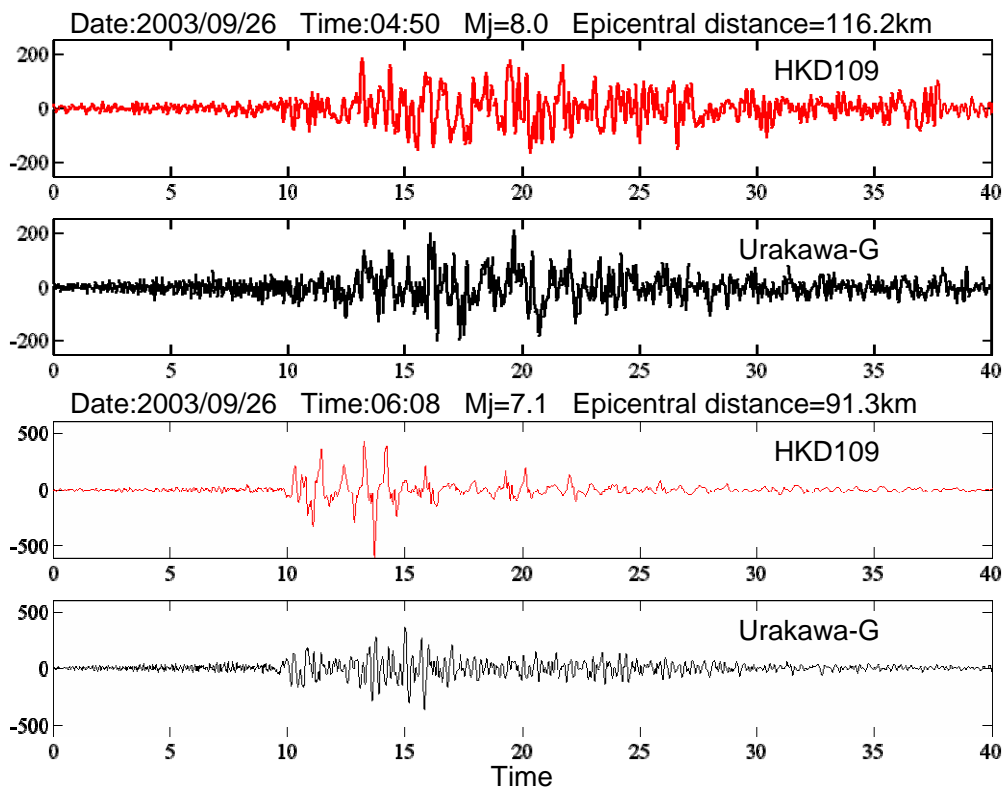


Figure 10. Upper: Acceleration time histories at HKD109 and Urakawa-G during the main shock. Lower: Acceleration time histories at HKD109 and Urakawa-G during the largest aftershock.

The PGA at Urakawa-G during the largest aftershock is about 1.7 times larger than that during the main shock, while the PGA at HKD109 during the largest aftershock is about 3.2 times larger than that during the main shock. Consequently the PGA of HKD109 is 1.9 times larger than that of Urakawa-G

during the largest aftershock. These observations indicate that the nonlinear response with the spiky waveform results in larger PGA compared with the linear response; the linear response requires nearly the same PGA at the two stations as observed during the main shock (the upper in Fig. 10). This nature is different from the nonlinearity observed at Toyokoro as mentioned above. According to Iai and Tobita (2006), we may call the Toyokoro case mild nonlinearity and the Urakawa case distinctive nonlinearity.

CONCLUSIONS

We have examined spatial distributions of velocity responses (damping factor of 5%) with various natural periods for the 2003 Tokachi-oki earthquake by using the dense strong-motion network data. We have found that the short-period ($T=0.1\text{sec}$) velocity response distribution is affected by the S-wave attenuation structure beneath north Japan; that is, the path effect, and that the long-period ($T=20\text{sec}$) one is mainly affected by the radiation pattern of Rayleigh waves, that is, the source effect. We have also found various types of the site effect; basin transduced surface waves in the large sedimentary basins, and nonlinear site responses at soft soil sites. However, this study is a qualitative one. We have to make a quantitative study of the source, path, and site effects for predicting strong ground motions from future large earthquakes.

ACKNOWLEDGEMENTS

K-NET, KiK-net strong-motion data were provided by National Research Institute for Earth Science and Disaster Prevention (NIED). The strong-motion data were also provided by JMA (Japan Meteorological Agency) and PARI (Port and Airport Research Institute). The deep underground structure data is constructed by NIED. Some of the figures in this paper were made using GMT (Wessel and Smith, 1995). This work was supported in part by the Grant-in-Aid for Scientific Research No. 16310120 from the Ministry of Education, Culture, Sports, Science and Technology, Japan.

REFERENCES

- Aoi, S., Obara, K., Hori, S., Kasahara, K., and Okada, Y., "New strong-motion observation network: KiK-net," *EOS Trans. AGU* 81, F863, 2000.
- Cervený, V., Molotkov, I. A., and Psencik, I., "Ray Method in Seismology," 214 pp., Univerzita Karlova, Praha, 1977.
- Hartzell, S., Bonilla, L.F., and Williams, R.A., "Prediction of nonlinear soil effects," *Bull. Seism. Soc. Am.*, 94, 1609-1629, 2004.
- Iai, S., Morita, T., Kameoka, T., Matsunaga, Y., and Abiko, K., "Response of a dense sand deposit during the 1993 Koshi-oki earthquake," *Soil and Foundations*, 35, 115-131, 1995.
- Iai, S., and Tobita, T., "Soil non-linearity and effects on seismic site response," *Proc. of the Third Inter. Sym. on effects of surface geology on seismic motion*, Grenoble, France, 30 August – 1 September 2006, 21-46, 2006.
- Kawase, H., "Review: Amplification of seismic waves by sedimentary layers and its simulation," *Zisin* 2, 46, 171-190, 1993 (in Japanese).
- Kinoshita, S., "Kyoshin Net (K-NET)," *Seismological Research Letters*, 69, 309-332, 1998.
- Maeda, T., and Sasatani, T., "Effects of the anomalous upper mantle structure on strong ground motion," *Geophys. Bull. Hokkaido Univ.*, No. 64, 91-113, 2001 (in Japanese).
- Maeda, T., and Sasatani, T., "Two-layer Q_s structure of the Slab near the Southern Kurile trench," *Earth Planets Space*, 58, 543-553, 2006a.

- Maeda, T., and Sasatani, T., "Long-period ground motions with a period of about 20 seconds from the 2003 Tokachi-oki earthquake," *Geophys. Bull. Hokkaido Univ.*, No. 69, 175-190, 2006b (in Japanese).
- Satoh, T., Sato, T., and Kawase, H., "Nonlinear behaviour of soil sediments identified by using borehole records observed at the Ashigara valley, Japan," *Bull. Seism. Soc. Am.*, 85, 1821-1834, 1995.
- Suzuki, H., Iwamoto, K., Morino, M., Shinohara, H., Fujiwara, H., Aoi S., and Hayakawa, Y., "Modeling subsurface structure for seismic hazard map in Hokkaido area," *Proceeding of the 111th Society of Exploration Geophysicists Japan*, 49-52, 2004 (in Japanese).
- Takai, N., Shimizu, G., and Okada, S., "New attenuation formula of earthquake ground motions passing through the volcanic front." *Proc. of the 13th World Conference on Earthquake Engineering CD-ROM*, 731, 2004.
- Wen, K.L., Beresnev, I.A., Yeh, Y.T., "Non-linear soil amplification inferred from downhole strong seismic motion data," *Geophys. Res. Lett.*, 21, 2625-2628, 1994.
- Wessel, P., and Smith, W.H., "New version of the Generic Mapping Tools released," *EOS Trans. AGU*, 329, 1995.